Methane Chemistry in the Hot Supersonic Nozzle

L. Romm,[†] Y. H. Kim,[‡] and G. A. Somorjai*[,†,§]

Lawrence Berkeley Lab, Department of Materials Science, Berkeley, California, Catalysis Center for Molecular Engineering, Korea Research Institute of Chemical Technology(KRICT), Yusong, Taejon, Korea, and Department of Chemistry, University of California, Berkeley, Calfornia

Received: January 29, 2001

Combination of pyrolysis and expansion to a supersonic molecular beam is shown to be very effective in conversion of pure methane to heavier hydrocarbons. The conversion reaches ~70% in the supersonic nozzle made of quartz with the diameter of orifice equal 100 μ. The major products are acetylene, benzene and its homologues. Free radicals are also detected in the product distribution. The mechanism consists of the surface generation of the radicals, C−C bond formation, desorption to the gas phase, and expansion to the supersonic beam. It is suggested that relatively short gas−surface contact time (about 50 ms at $T_{\text{nozzle}} = 1000$ °C) enables simultaneous kinetic and thermodynamic control.

1. Introduction

Great industrial interest in methane as a potential dominant future source for the synthetic replacement of petroleum-derived hydrocarbons has long been a driving force for the research and development of methane-coupling techniques to form the higher hydrocarbon products. There are two major methods of the direct conversion of methane to heavier hydrocarbon products: catalytic oxidative coupling and high-temperature pyrolysis. The oxidative condensation involves heterogeneous catalysis over a variety of metal oxides[1−3] at optimal temperature range 550−850 °C. The process is characterized by above 50% CH_4 conversion and yields a considerable amount of C_2 hydrocarbons. However, the selectivity to ethane and ethylene decreases with the increase of the methane conversion rate. Of course, the simultaneous formation of CO, CO_2, and water is unavoidable.

Thermal steady state pyrolytic dehydrogenation of methane is favorable only at temperatures above 1200 °C.[2,4] The dominant product of this process is acetylene due to the decrease of its free energy of formation at higher temperatures. However, acetylene is less stable than its constituents at this temperature and readily decomposes to carbon deposited on the surface and hydrogen in the gas phase. Thus, the stabilization of acetylene, and possibly longer chain hydrocarbons that may form from acetylene, requires a very short contact time of methane with the reactor walls for the rapid desorption and cooling of the products. Thus, kinetic rather than thermodynamic control over the high-temperature self-coupling of methane must be established.

Expansion of a gas through a hot nozzle orifice to form a supersonic molecular beam is thought to be an appropriate experimental technique to overcome the thermodynamic limitations of the steady-state equilibrium conditions. During pyrolysis, very fast transition of a compressed gas to free-molecular flow during the supersonic expansion provides sufficient cooling of the internal molecular degrees of freedom[5,6] along with a withdrawal of the molecules to vacuum to enable their detection and analysis. D. Herschbach and co-workers[7,8] recently utilized this approach to demonstrate facile formation of higher hydrocarbons from ethane in the heated supersonic nozzle beam. Flowing through 1000 °C nickel nozzle, ~60% of the reactant ethane was converted to $C_3 \div C_{12}$ unsaturated hydrocarbons within 10 ms contact time. However, no conversion of methane was observed under similar conditions.[8] Work in our laboratory has shown that ethane conversion can be increased to almost 100%.[9] We were also able to detect higher hydrocarbons formed from methane in the hot (1150 °C) nozzle made of quartz with the orifice diameter of about 200 μ.[9] The product distribution from methane resembled that from ethane. The direct nonoxidative conversion of methane was estimated to be equal to 20% within 10 ms.

In this paper, we report much larger (up to 70%) conversion of methane to longer chain hydrocarbons in the hot quartz nozzle with the orifice diameter of 100 μ. No self-coupling of methane to the heavier products was detected in the metal nozzles (Ni, Mo, Fe) ≤1000 °C, whereas at higher temperatures, the metal nozzles rapidly clogged with soot and, possibly, metal carbides. The product distribution from methane presents a variety of higher hydrocarbon molecules with number of carbon atoms in the range of 2 to 12. The intensity of the peaks with even number of carbon atoms is somewhat higher,[7−9] than the peaks with odd number.

The mechanism of the chemical process is discussed in terms of the formation of precursor free radicals from methane, which are generated and react on the surface followed by the desorption to the gas phase and supersonic expansion. We detected methyl (CH_3) and propargyl (C_3H_3)[7,8] free radicals in the supersonic beam. An attempt was made to form products other than hydrocarbons. For this purpose, we added either oxygen or NO or CO_2 to the reactant methane. However, no hydrocarbon derivatives could be detected among the hot nozzle reaction products.

A time-of-flight (TOF) technique was employed to determine the nozzle temperature because it is not possible to measure, without sizable error, high temperatures of the quartz nozzles using a standard thermocouple method. The TOF technique

[†] Lawrence Berkeley Lab, Department of Materials Science.
[‡] Catalysis Center for Molecular Engineering, Korea Research Institute of Chemical Technology(KRICT).
[§] Department of Chemistry, University of California.

10.1021/jp010366d CCC: $20.00
Published on Web 06/28/2001

provides a reliable estimation of the nozzle orifice temperature based on the measurement of velocity distribution of a supersonic beam constituents.[6,10]

2. Experimental Section

Detailed description of our experimental setup has been given elsewhere.[9] Briefly, a CW supersonic molecular beam is generated in the source chamber, propagates to the 1st differentially pumped chamber through a skimmer and enters the 2nd detection chamber through an additional collimating aperture that is placed between the detection and the 1st differentially pumped chamber. The quadrupole mass spectrometer (QMS) detector was placed in the detection chamber in the line-of-sight of the beam. Base pressure in the detection chamber was maintained at less than 1×10^{-9} Torr.

We used nozzles fabricated from quartz with the orifice diameter of $100 \pm 10\ \mu$ throughout the entire set of experiments reported here. We tried two different shapes of nozzles: bird beak-like and that similar to the metal nozzles used previously.[9] We did not find a significant difference within uncertainties of our experimental setup. The manufacturing of quartz nozzles is fast, easy, and inexpensive, whereas the orifice diameters can be readily reproduced within the control limits of $10\ \mu$.

We employed TOF method to measure the nozzle temperature. Helium was flowed through the nozzle prior to and after the experiments with CH_4 or gas mixtures at the same conditions of the nozzle heating. We monitored the temperature stability of the outer nozzle wall in the heating zone using K-type thermocouple. Normally, the thermocouple reading was stable within 2 degrees, when methane (or a gas mixture) was switched to helium and conversely. A tiny synchronous gyro-motor (Condor Pacific Ltd., Israel) carrying a chopper wheel was placed in the 1st differentially pumped chamber. Solid 0.5 mm thick stainless steel wheel has two 0.5 mm wide slits cut opposite each other. The motor was attached to the linear transfer mechanism to enable the insertion of the wheel into the beam of molecules emerging from the source chamber. Typical rotation rate was 320 Hz, as was measured by an optocoupler with very fast rise time. The optocoupler also served as a trigger for the detection of the time of arrival at the QMS.

A Digital oscilloscope was used to record the time of arrival signal directly from the secondary electron multiplier of the QMS via a homemade fast (2 μs rise time) preamplifier. The spectra were stored on the floppy disk and analyzed afterward to determine the nozzle temperature. After the ion time-of-flight inside the QMS filter was subtracted from the raw data, the time of arrival spectra were converted to velocity distribution spectra using Jacobian[10] $d\upsilon/dt = |L/t^2|$, where L is a distance between chopper wheel and QMS ionizer; L = 72.1 cm.

Experimental distributions of the velocity of the helium beam $F(\upsilon)$ were then fit by the modified Maxwellian function for a supersonic beam,[10,11] as follows

$$F(\nu) \propto \nu^3 \cdot e^{-m_{He}(\nu-\nu_0)^2/2kT_{||}} \qquad (1)$$

where υ_0 is the terminal velocity of the beam, $T_{||}$ describes velocity spread relative to υ_0 along the beamline. Then, the mean square velocity $\langle \upsilon^2 \rangle$ was calculated using the fit parameters, and the nozzle temperature was established through the expression 2[6]

$$T_{\text{nozzle}} = \frac{\gamma_{\text{He}} - 1}{\gamma_{\text{He}}} \cdot \frac{m_{\text{He}} \langle \nu^2 \rangle}{2k} \qquad (2)$$

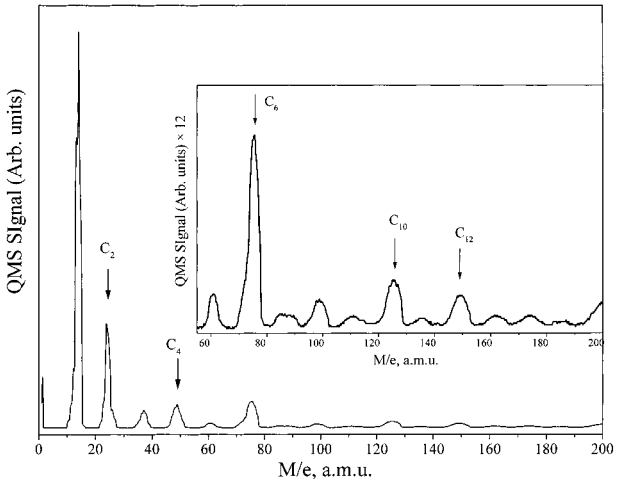

Figure 1. Typical low resolution mass spectrum of the products from the pure methane at $T_{\text{noz}} = 1066$ °C, $P_{\text{upstream}} = 215$ Torr. The nozzle was made of quartz and has a 100 μ orifice. Some peaks are marked by the number of carbon atoms. Inset presents detailed product distribution of the masses above 55 amu.

where $\gamma_{\text{He}} = C_P(\text{He})/C_V(\text{He}) = {}^5/_3$. The accuracy of the TOF nozzle temperature measurement was estimated to be ± 50 degrees at $T_{\text{noz}} = 1000$ °C.

All gases used in the present work (CH_4, He, O_2, NO, CO_2) were of nominally high (99.99%) and ultrahigh purity, and no impurities were observed by QMS within our experimental detection limits. All of the mass spectra were refined by subtraction of the corresponding background gas signal from the raw mass spectra. Background gas mass spectra were taken when the beam was on and cut from the QMS by a shutter.

The nozzles were cleaned up in situ by flowing oxygen at $T_{\text{noz}} > 700$ °C. We used the same technique to burn surface carbon and unclog the nozzle when necessary.

3. Results

3.1. Methane Conversion. A discernible signal in the C_2 region of the mass spectrum appeared when the nozzle temperature reached ~950 °C ÷ 1000 °C. The C_m ($m \geq 2$) hydrocarbon signals became stronger with the temperature up to ~1100 °C and leveled off in the range 1100 ÷ 1150 °C. Above 1150 °C, the rate of surface carbon deposition (probably soot) exceeded the rate of methane coupling, and the nozzle clogged. A typical low resolution mass spectrum of the products of nozzle methane conversion is shown in Figure 1. The product distribution essentially resembles qualitatively that from pure ethane,[7−9] indicating the same mechanism of conversion.

High-resolution mass spectrum of the 1−35 amu region, taken under the same conditions as that in Figure 1, is presented in Figure 2. Major contribution to the intensity of the C_2 signal comes from acetylene, the formation of which is thermodynamically favorable.[2,12] Weak peaks at 27 and 28 amu are also seen, indicating the presence of small amount of ethylene, the formation of which during methane pyrolysis is thermodynamically favorable[13] under 1000 °C. Note an unusually high ratio of the intensities of peaks 15 and 16 amu.

Conversion of methane to higher hydrocarbons changes at 1066 °C from about 60% at $P_{\text{upstream}} = 50$ Torr to almost 70% at $P_{\text{upstream}} = 215$ Torr. At higher pressures the rate of methane decomposition $CH_4 \rightarrow C(s) + 2H_2(g)$ is apparently higher than the rate of formation of acetylene and other products due to longer contact time, and the nozzle rapidly clogs with carbon. Pressure dependence of the yields of various products is shown

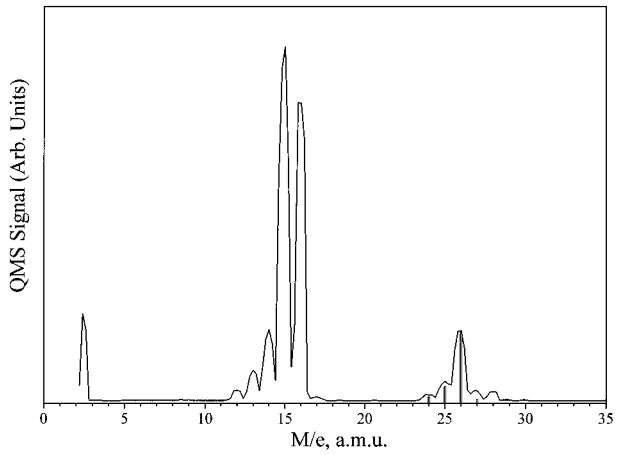

Figure 2. High-resolution mass spectrum of 0 to 35 amu region for the same reaction conditions as in Figure 1. Bargraph shows a reference spectrum of acetylene. Discernible peaks at 27 and 28 amu may be identified as originated from ethylene.

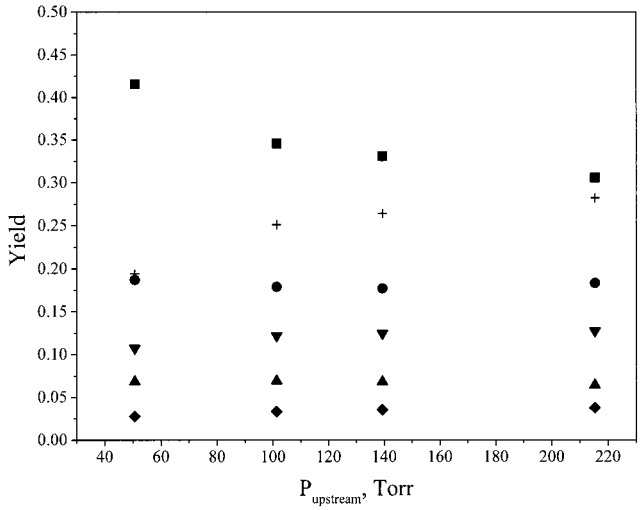

Figure 3. Yields of some products of methane beam reaction in the quartz supersonic nozzle at T_{nozzle} = 1066 °C as a function of the stagnation pressure. ■ denote C_1 products, ● − C_2, ▲ − C_3, ▼ − C_4, ◆ − C_5, and + − C_6.

in Figure 3. Although the yield of C_2 − C_5 products practically does not change with the stagnation pressure, the C_6 (benzene[7−9]) yield rises from 20% at $P_{upstream}$ = 50 Torr to 28% at $P_{upstream}$ = 215 Torr. Selectivity to benzene increases from 33% to 41% within this pressure range, whereas that for the C_2 products (apparently acetylene and ethylene) drops from 32% to 26%. Because it is not possible to separate fragmentation patterns of some of the products from the parent peaks of others in the same region of the mass spectrum, the calculations of the yields and selectivities are semiquantitative and serve as an estimation of the reaction kinetics. These calculations are based on the area-under-peak measurements and carbon atom balance. No coke formation in the nozzle is allowed for. Because of our lack of ability to resolve certain mass signals, no additional special calibration of the QMS sensitivities has been done.

The deactivation of the nozzle strongly depends on the temperature and stagnation pressure. Usually, higher T_{noz} and $P_{upstream}$ values lead to rapid nozzle degradation and clogging with carbon. Unlike metal nozzles, we were able to recover the chemical activity of the quartz nozzle by flowing oxygen. Gaseous CO and CO_2 were formed and evacuated from the nozzle into the vacuum system. At moderate temperatures and lower $P_{upstream}$ (shorter contact time), the nozzle lifetime was much longer. Figure 4 shows the yield trends for various products of the methane conversion at $T_{noz} \approx$ 1000 °C and $P_{upstream}$ = 63 Torr. Integral intensity of the products (not shown) was measured to be half as much after about 3.5 h of the continuos run.

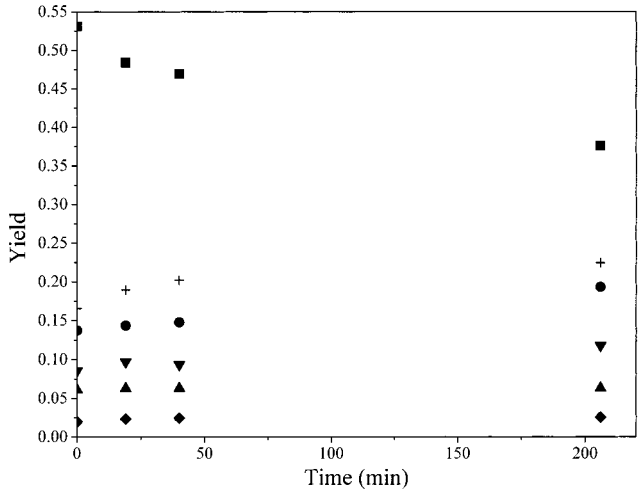

Figure 4. Yield trends of the products of pure methane conversion at T_{noz} = 1000 °C and $P_{upstream}$ = 63 Torr. The products are marked as in Figure 3.

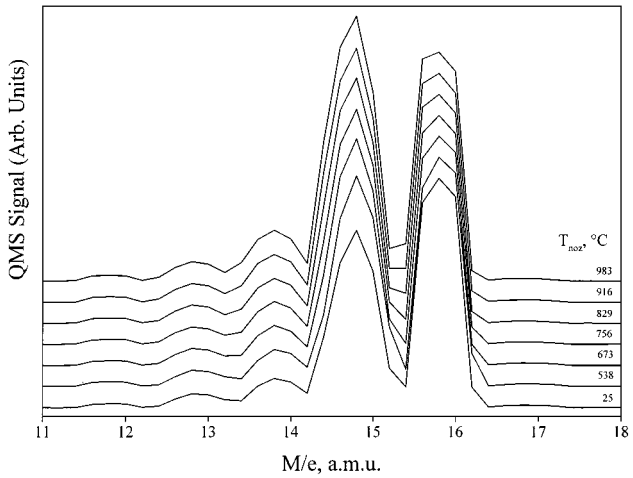

Figure 5. High-resolution mass spectra of C_1 region, taken at different temperatures of the nozzle, through which pure methane was flowed at $P_{upstream}$ = 90 Torr.

3.2. Formation of C_1 Radicals. As it was mentioned, the experimentally observed signal in the C_1 mass region comprises possibly the contributions from methane and other C_1 products. In pure CH_4, the mass spectrum fragmentation pattern at mass 15 (CH_3^+) is only 83% of the 16 amu parent peak intensity (UTI 100 QMS, Electron impact energy is −70 eV). This is illustrated in Figure 5 by the lowest curve obtained for a methane nozzle beam at room temperature. As the T_{noz} was increased, the intensities of masses 12 through 15 gradually increased relative to mass 16. Figure 5 demonstrates this experimental observation. All spectra were normalized to mass 16 peak.

An enhancement of the signals from masses 12 to 15 is likely due to formation of methyl radicals in the hot nozzle.[14−16] Relative intensities of these radicals in the beam were obtained by subtraction of the pure methane signal (obtained at T_{noz} = 25 °C, Figure 5) from every measured raw spectrum. The corresponding curves are shown in Figure 6. We argue that peaks in Figure 6 belong to methyl radicals and their cracking patterns rather than derive from fragmentation patterns of

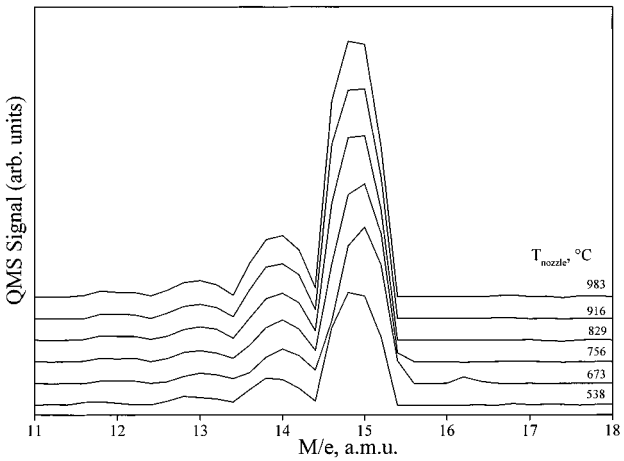

Figure 6. High-resolution mass spectra of methyl radicals, produced from methane in the heated supersonic nozzle at $P_{upstream} = 90$ Torr. The curves were obtained by subtraction of pure methane mass spectrum, taken at $T_{noz} = 25$ °C (lowest curve in Figure 5), from the spectra, taken at higher nozzle temperatures. The subtraction followed the normalization to the mass 16 intensity.

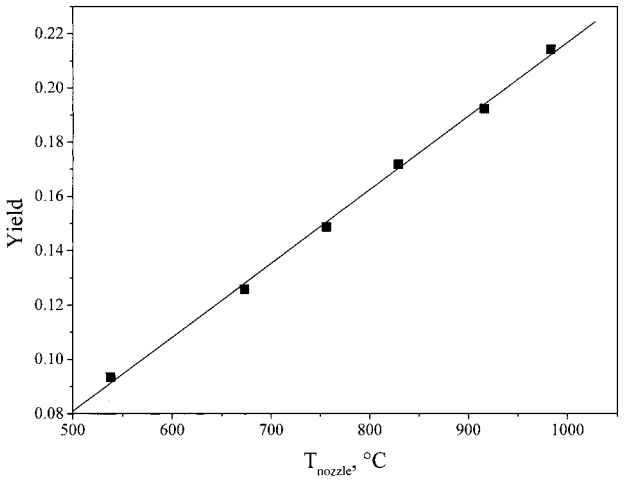

Figure 7. Yield of the methyl radical production as a function of the nozzle temperature. The yield values are calculated relative to methane, no higher hydrocarbons were taken into account.

methane. The intensities of the signals from CH and CH_2 radicals were below our detection limit, as was verified by the variation of the electron impact energy[15] from −25 to −100 eV.

It is unlikely that the fragmentation upon electron impact in the ionizer is coupled with the vibrational excitation of methane molecules in the supersonic beam, emerging from the heated nozzle. An effect of the translational energy activation may also be ruled out as a possible source for the changing cracking patterns of methane in the mass spectrum. The CH_4 molecule spends even less time in the ionizer when emerges from the heated nozzle in contrast to the room-temperature nozzle. Thus, extra cracking by electron impact in the QMS ionizer is unfavorable and unlikely.

The yield of the methyl radicals is shown in Figure 7, as a function of the nozzle temperature. The relative concentration of the free radicals in the supersonic molecular beam increases linearly with nozzle temperature and reaches values above 20% relative to unreacted methane. Note that the signal from methyl radicals is noticeable even at low T_{noz}, when no higher hydrocarbons are formed. This observation may be rationalized by CH_3/CH_4 equilibrium thermodynamics considerations.[2,17]

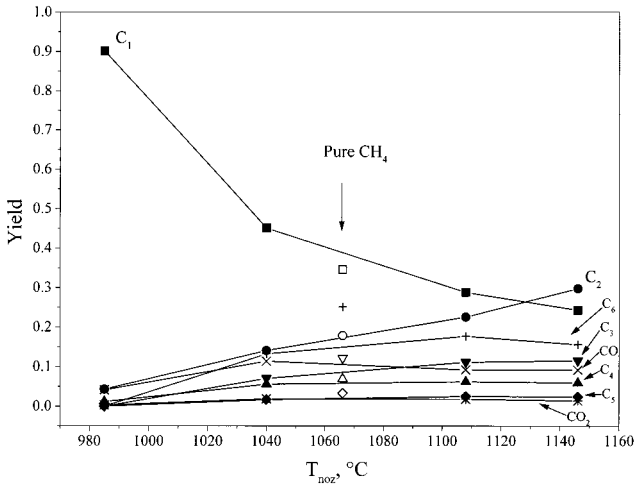

Figure 8. Yield of different products from CH_4/O_2 mixture with 20% vol. of oxygen as a function of the nozzle temperature at $P_{upstream} = 102$ Torr. The products are marked as follows: ■, − C_1, ● − C_2, ▼- C_3, ▲- C_4, ◆- C_5, + − C_6, × − CO, * − CO_2. Open symbols belong to the products of pure methane conversion. The shapes of these symbols correspond to the filled ones.

3.3. Reactivity of CH_4/O_2, CH_4/NO, and CH_4/CO_2 Mixtures. As we were able to observe the direct nonoxidative reactivity of pure methane in the hot supersonic nozzle, we made an attempt to probe oxidative methane coupling. For this purpose, we used different mixtures of methane with oxidizers O_2, NO, and CO_2. To our surprise, methane chemistry, when in the mixture essentially reproduced that of the pure methane under similar reaction conditions. We were not able to synthesize hydrocarbon derivatives, nor could we improve the yields and selectivities to the longer chain hydrocarbons. Figure 8 presents the temperature dependence of the yield of various products from the mixture of CH_4 and O_2 in proportion approximately 4 to 1. The data on the yield of higher hydrocarbons from pure methane is given for the comparison.

Mass spectra of the products from pure methane and from the gas mixtures feed looked similar at the same nozzle conditions, except the presence of H_2O, CO, and CO_2 peaks for the mixtures. Oxygen reacts predominantly with hydrogen and surface carbon, which are the products of the decomposition of methane. Formation of water indicates release of hydrogen during the oligomerization of methane in the quartz nozzle. Quantitative analysis of the rate of hydrogen formation during the course of reaction in the nozzle is not possible due to the poor performance of our mass spectrometer in the H_2 mass region. Selective interaction of oxygen with surface carbon can account for our ability to run reactions of mixtures at higher nozzle temperatures for longer times as compared with pure methane as a reactant. In fact, the mixture of methane with oxygen in proportion ∼4:1 (ratio by volume) taken as a feed gas exhibits essentially the same reactivity under similar nozzle conditions as pure methane relative to the formation of higher oxygen-free hydrocarbons. However, the great advantage of using oxygen was the ability to carry out the reaction continuously for about 3−4 h at T_{noz} above 1100 °C, whereas for pure methane, nozzle clogging occurs within minutes under the same conditions. The disadvantage of using oxygen-methane mixtures is the formation of considerable amount of water, CO and CO_2. CO signal was twice as high as that of acetylene at $T_{noz} > 1100$ °C, the signal from water has roughly the same intensity as that from acetylene. The rate of formation of CO_2 was measured qualitatively to be much lower than that of CO and comparable

with that of benzene (no carbon atom balance was taken into account).

4. Discussion

We propose that the formation of higher hydrocarbons from pure methane occurs essentially by the same mechanism as that from ethane.[7−9] This includes (1) a generation of free radicals on the hot surface of the nozzle[14] via hydrogen atom(s) abstraction,[16] (2) desorption to the gas phase or C−C bond formation by oligomerization and desorption to the gas phase. Desorption is thought to be caused by both the thermal activation of the desorbing species and the intensive flow inside the nozzle.[7,8] We believe we were able to observe the hot nozzle reactivity of methane in contrast to previous studies[7,8] due to application of quartz as a nozzle material and decreasing the nozzle orifice diameter. Quartz, unlike metals, is relatively inert to surface carbide formation at high temperatures. This process, along with the deposition of carbon, leads to the rapid degradation and clogging of metal nozzles. The smaller nozzle orifice lengthens contact time within the hot reaction zone. We calculated the contact times following Shebaro[18] and obtained values in the range of 30 to 100 ms for different stagnation pressures and $T_{noz} = 1000$ °C. These contact times are sufficiently long to produce thermodynamically unfavorable (as compared with C and H_2) heavier hydrocarbons as reaction intermediates, that desorb and expand in the supersonic beam and exit in a vacuum where they are detected by mass spectrometry. These contact times are too short for methane, however, to decompose completely to carbon and hydrogen inside the nozzle. At the nozzle temperatures used in the current study, acetylene and benzene are the most stable hydrocarbons.[17] Moreover, their Gibbs free energy of formation decreases with increasing temperature. This may account for the experimental observation that their intensities are strongest among the products (see Figures 1, 3, 4, 8).

Free radical mechanism of the formation of higher hydrocarbons from methane is clearly illustrated by the experimental observation of methyl radicals as supersonic beam constituents. Short contact time within the nozzle and small number of collisions between the reactive molecules[6] makes the survival of the methyl radicals possible prior to the expansion to the supersonic beam, as detected by the QMS. The number of collisions rises with the nozzle temperature. However, the rate of reaction of the nascent products (e.g., ethane) also increases.[8]

Our findings, that the addition of oxygen or other oxygen containing gases to methane neither boosts the conversion rate nor leads to the formation of hydrocarbon derivatives, are supported by theoretical studies of equilibrium methane pyrolysis.[19] Catalytic rather than pyrolytic approaches should be used in order to achieve discernible rates of the formation of oxygen containing hydrocarbon products. Quartz is apparently a poor catalyst and should be substituted with metal oxides.[2,20]

Selective interaction of oxygen with surface carbon when added to methane, stresses the surface mediated mechanism of the nozzle beam reaction. Previously, in our experiments with ethane, we seeded C_2H_6 in Ar in proportion 1 to 10. The rate of the formation of benzene was measured to be even slightly higher than that for pure ethane as a reactant under the same nozzle conditions. The C_6H_6 signals were compared after normalization to the intensity of acetylene signal. This experimental observation indicates that the process of oligomerization occurs predominantly on the surface of the hot nozzle.

It may be suggested that C−C bonds are formed on the nozzle surface via the coupling of CH_m ($m = 1,2$) radicals, which we were not able to detect in the beam composition. The rate of formation of these radicals increases with the nozzle temperature such, that adequate amount can be produced within the contact time of methane. Thermodynamically, this enables the formation of the more stable acetylene, benzene and its higher homologues. The rate of their decomposition is apparently slower than the rate of desorption and expansion to the supersonic beam. Thus, interplay between thermodynamic and kinetic regimes makes possible the production of higher hydrocarbons from methane with considerable rates in the hot supersonic nozzle. Understanding the details of such the interplay will help to explore the ways to establish control over the selectivities to certain products. Pyrolysis coupled with the supersonic flow is a relatively poorly studied area of reaction chemistry, and we are unable at this point to discuss specific elementary chemical processes involved in the overall reaction mechanism. Probably, modification and optimization of the nozzle design may lower a concentration of unreacted CH_3 radicals and, consequently, drive the reaction toward the formation of more C_2 or C_6 hydrocarbons.

5. Summary

Conversion of pure methane reached 70%, when it reacted in a hot (1000−1150 °C) supersonic nozzle made of quartz with the orifice diameter of 100 μ. Major products in the distribution were hydrogen, acetylene, benzene, methyl, and propargyl radicals, but other hydrocarbons were also detected. Addition of O_2, NO or CO_2 did not enhance methane conversion rate as oxygen reacts primarily with surface carbon formed by methane decomposition. No oxygen containing hydrocarbon derivatives were detected. The lifetime of the nozzle was longer compared with pure methane as a reactant as a result of surface carbon removal by oxygen.

The mechanism has apparently involved pyrolytic rather than catalytic surface generation of free hydrocarbon radicals with subsequent coupling to heavier hydrocarbon products prior to desorption to the gas phase and expansion to the supersonic beam. This predominantly surface mediated mechanism is probably dictated by the delicate interplay between kinetic and thermodynamic regimes of the formation of higher hydrocarbons.

Acknowledgment. We would like to thank Prof. M. Asscher for providing us with the chopper motor, and Dr. Y. Gotkis, Dr. L. Baranov, Dr. Y. Borodko, and especially Dr. S. H. Kim for very helpful and stimulating discussions. This work was supported by the Director, Office of Energy research, Office of Science, Division of Materials Sciences, of the U.S. Department of Energy under Contract No. DE-AC03-76SF00098.

References and Notes

(1) *Methane Conversion by Oxidative Processes: Fundamental and Engineering Aspects*; Wolf, E. E., Ed.; Van Nostrand Reinhold: New York, 1992.

(2) Olah, G. A.; Molnár, Á. *Hydrocarbon Chemistry*; John Waley & Sons Inc.: New York, 1995.

(3) Fox, J. M. *Catal. Rev. − Sci. Eng.* **1993**, *35*(2), 169.

(4) Back, M. H.; Back, R. A. in *Pyrolysis: Theory and Industrial Practice*; Albright, L. F., Crynes, B. L., Corcoran, W. H., Eds.; Academic Press: New York, 1983.

(5) Anderson, J. B.; Andres, R. P.; Fenn, J. B.; Maise, G. "Studies of Low-Density Supersonic Jets", In *Rarefied Gas Dynamics*; de Leeuw, J. H., Ed.; Academic Press: New York, London, 1966; Supplement 3, V2, 106.

(6) Miller, D. R. In *Atomic and Molecular Beam Methods*; Scoles, G., Ed.; Oxford University Press: Oxford, 1998; Volume 1; Chapter 2, 14.
(7) Shebaro, L.; Abbott, B.; Hong, T.; Slenczka, A.; Friedrich, B.; Herschbach, D. *Chem. Phys. Lett.* **1997**, *271*, 73.
(8) Shebaro, L.; Bhalotra, S. R.; Herschbach, D. *J. Phys. Chem. A* **1997**, *101*, 6775.
(9) Romm, L.; Somorjai, G. A. *Catalysis Lett.* **2000**, *64* (2−4), 85.
(10) Auerbach, D. J. In *Atomic and Molecular Beam Methods*; Scoles, G., Ed.; Oxford University Press: Oxford, 1988; Volume 1; Chapter 14, 362.
(11) Janda, K. C.; Hurst, J. E.; Becker, C. A.; Cowin, J. P.; Auerbach, D. J.; Wharton, L. *J. Chem. Phys.* **1980**, *72*(4), 2403.
(12) Duff, R. E.; Bauer, S. H. *J. Chem. Phys.* **1962**, *36*, 1754.
(13) Arutyunov, V. S.; Vedeneev, V. I.; Moshkina, R. I.; Ushakov, V. A. *Kinetika i Kataliz* **1991**, *32*(2), 267.
(14) Kohn, D. W.; Clauberg, H.; Chen, P. *Rev. Sci. Instrum.* **1992**, *63*(8), 4003 and references therein.
(15) Peng, X.-D.; Viswanathan, R.; Smuddle, G. H., Jr.; Stair, P. C. *Rev. Sci. Instrum.* **1992**, *63*(8), 3930.
(16) Driscoll, D. J.; Lunsford, J. H. *J. Phys. Chem.* **1985**, *89*, 4415.
(17) Guéret, C.; Daroux, M.; Billaud, F. *Chem. Eng. Sci.* **1997**, *52*(5), 815.
(18) Shebaro, L. *Ph.D. Dissertation*, Boston College, 1996.
(19) Larkins, F. P.; Khan, A. Z. *Aust. J. Chem.* **1989**, *42*, 1655.
(20) Miremadi, B. K.; Colbow, K.; Morrison, S. R. *Can. J. Chem.* **1997**, *75*, 465.